HHS Public Access

Author manuscript

J Cell Physiol. Author manuscript; available in PMC 2020 November 01.

Published in final edited form as:

J Cell Physiol. 2019 November ; 234(11): 19824–19832. doi:10.1002/jcp.28581.

Osteocytic Connexin 43 Channels affect Fracture healing

Yunhe Chen[#a], **Meng Chen**[#a], **Tong Xue**[a], **Guobin Li**[a], **Dongen Wang**[a], **Peng Shang**[c], **Dr. Jean X. Jiang**[d,*], **Huiyun Xu**[a,b,c,*]

[a]Key Laboratory for Space Bioscience and Biotechnology, School of Life Sciences

[b]Research Center of Special Environmental Biomechanics & Medical Engineering, Northwestern Polytechnical University, Youyi Xilu 127, Xi'an, Shaanxi 710072, China

[c]Key Laboratory for Space Bioscience and Biotechnology, Research & Development Institute in Shenzhen, Northwestern Polytechnical University, Gaoxin Fourth South Road 19, Shenzhen, Guangdong 518057, China

[d]Department of Biochemistry and Structural Biology, University of Texas Health Science Center, San Antonio, TX 78229, USA

[#] These authors contributed equally to this work.

Abstract

The cross-talk between cells is very critical for moving forward fracture healing in an orderly manner. Connexin (Cx) 43-formed gap junctions and hemichannels mediate the communication between adjacent cells and cells and extracellular environment. Loss of Cx43 in osteoblasts/osteocytes results in delayed fracture healing. For investigating the role of two channels in osteocytes in bone repair, two transgenic mouse models with Cx43 dominant negative mutants driven by a 10kb-DMP1 promoter were generated: R76W (gap junctions are blocked, while hemichannels are promoted) and Δ130–136 (both gap junctions and hemichannels are blocked). R76W mice (promotion of hemichannels) showed a significant increase of new bone formation, while a delayed osteoclastogenesis and healing was observed in Δ130–136 (impairment of gap junctions), but not in R76W mice (hemichannel promotion may recover the delay). These results suggest that gap junctions and hemichannels play some similar and cooperative roles in bone repair.

Keywords

Cx43; gap junction; hemichannel; transgenic mouse model; fracture healing

[*]Corresponding authors: Dr. Huiyun Xu, Key Laboratory for Space Biosciences and Biotechnology, School of Life Sciences, Northwestern Polytechnical University, Xi'an, Shaanxi 710072, China. celldon@nwpu.edu.cn, Dr. Jean X. Jiang, Department of Biochemistry and Structural Biology, University of Texas Health Science Center, San Antonio, TX, USA. jiangj@uthscsa.edu.

AUTHOR CONTRIBUTIONS

H.X. and J.X.J. contributed to the conception and design of the study, prepared the manuscript and made a revision of the manuscript. Y.C. and M.C. designed the study, conducted the experiment, analyzed the data, drafted and revised the manuscript. T.X., G.L. and D.W. analyzed the data. P.S. designed the study. All the authors participated in discussion and editing of the manuscript.

CONFLICT OF INTERESTS

All authors state that they have no conflicts of interest.

Introduction

Fracture healing is a complex regeneration process followed bone injury, which is artificially divided to four overlapped phases: inflammation, soft callus formation, hard callus formation, and remodeling. The dynamic process involves cross-talk of a variety of bone cells, inflammatory and vascular cells (Schindeler, McDonald, Bokko, & Little, 2008), also well-organized activiation including mesenchymal stem cells proliforation and differentiation to chondrocytes and osteoblasts, endochondral bone formation by chondrocytes, intramembranous ossification by osteoblasts, bone remodeling driven by osteoclasts and osteoblast (Marsell & Einhorn, 2011). But the role of osteocytes (about 90–95% of bone cells) in the process is still not clear.

Osteocytes are well-known as major orchestrator to regulate the function of various bone cells and maintain homeostasis of bone tissue (Bonewald, Kneissel, & Johnson, 2013). And the interaction between various bone cells is essential for fracture healing, a form of bone regeneration, suggesting that osteocytes may play a vital role in the process. K. Kusuzaki et al have shown that woven bone osteocytes may be necessary for attachment and maturation of lamellar bone osteocytes at an early stage of bone repair (Kusuzaki et al., 2000). Huang et al have shown that osteocytes orchestrate the new bone formation and remodeling in the electrotherapy for bone fracture (Huang, Chen, & Chen, 2008). In recent years, some studies have shown that antibodies of sclerostin (Sost) enhances fracture healing (Jawad et al., 2013; Ominsky et al., 2011), and Sost deficiency mice shows accelerated bone formation and strength in the callus (Li et al., 2011; McGee-Lawrence et al., 2013). Now that Sost is expressed specifically in osteocytes, these results also indicate the role of osteocytes in bone repair.

Also, communication of signal molecules between bone cells is very critical for moving forward fracture healing in an orderly manner (Tatsuyama, Maezawa, Baba, Imamura, & Fukuda, 2000). In bone tissue, connexin-formed gap junctions and hemichannels permit small molecules (<1kDa) to pass through, which play important roles in transfering signals between adjacent cells and cells and extracellular environment (Batra, Kar, & Jiang, 2012; Plotkin & Bellido, 2013). So connexin-formed channels may involve in regulating the communication between bone cells in different phases of fracture healing.

Connexin 43 (Cx43) is the most abundent connexin expressed in osteocytes (Civitelli, 2008). We have generated two transgenic mouse models with overexpression of Cx43 dominant negative mutants driven by a 10kb-DMP1 promoter: R76W (gap junctions are blocked, while hemichannels are promoted) and Δ130–136 (both gap junctions and hemichannels are blocked). Using the two mouse models, our previous study has shown the distinctive roles of gap junctions and hemichannels in maintaining bone structures, remodeling and material properties (Xu et al., 2015).

In the present study, we generated tibial fracture in R76W and Δ130–136 mice, and investigated the role of Cx43-formed gap junctions and hemichannels during healing, which may explore the clinical potential of Cx43 channels in bone repair.

Materials and Methods

Animals.

Two lines of transgenic models expressing dominant negative mutants of Cx43 in osteocytes, R76W and Δ130–136, were generated at the University of Texas Health Science Center at San Antonio (UTHSCSA). For R76W mice, function of gap junctions was inhibited, but hemichannels was promoted specifically, and for Δ130–136 mice, both of gap junctions and hemichannels were inhibited (Xu et al., 2015). Mice were housed on a 12-hour light/dark cycle, at 25°C, 40% relative air humidity with free access to water and feed. Genotyping was performed by real-time PCR using genomic DNA isolated from mouse toe. All animal protocols were approved by the Northwestern Polytechnical University (NPU) Institutional Animal Care and Use Committee.

Tibial fracture model

Ten-week-old male R76W, Δ130–136 and wild-type (WT) C57BL/C mice were anesthetized using EZ-AF90000 Auto Flow Rolent Anesthesia System, and left tibia was transected at the crest point using electric grinder (DREMEL 3000), with the fibula and surrounding tissue intact. Syringe needle was inserted into the bone marrow cavity through the tibial plateau to ensure the two broken ends of fractured tibia together. Right tibia was as the control. The mice were sacrificed at 7, 14, 21 and 28 days postoperatively and bone samples were harvested.

Micro-computed tomography analysis

Left tibia was isolated and kept in 80% alcohol at 4°C overnight after removing soft tissues. The 1.518-mm-long region of interest (ROI) above and below the fracture line was selected, and microarchitecture was detected by a high-resolution micro-CT (μCT) (Locus SP, GE) with a scanning resolution at 8 μm. In cortical area, 800 (193 mg/cm^3) was set as the threshold value of low bone density, and 1600 (385 mg/cm^3) was set as the high bone density. All analyses were performed using the MicroView program (GE Healthcare). The following parameters were analyzed by ABA-specific bone analysis software: Callus volume (BV), Bone Volume to Tissue Volume (BV/TV), Tissue Mineral Density (TMD), Trabecular Separation (Tb.Sp), Trabecular Thickness (Tb.Th) and Trabecular Number (Tb.N).

Biomechanical testing

Tibia specimen was assessed at 21 and 28 days post fracture. Three-point bending test was performed at either the fracture line or the same point of control tibia using the BOSE mechanical test system. The lower supports were 8 mm apart and the displacement rate was 1.2 mm/min to make bone failure. Maximum force and stiffness were calculated to assess recovery of tibial mechanical proporty.

Histology and Immunohistochemistry

Tibia was harvested at 7, 14, 21 and 28 days after fracture, and then fixed in 4% paraformaldehyde for 48 hours. The samples were decalcified with 10% ethylene diamine tetraacetic acid (EDTA) for 6 weeks prior to paraffin embedding. Serial sections (5 μm) were

stained with Safranin / Fast green and tartrate-resistant acid phosphatase (TRAP). The 1.518-mm-long ROI above and below the fracture line was selected, the area of cartilage and mineralized bone, and osteoclast number were calculated by Image J software (National Institutes of Health, USA).

Also paraffin sections of callus were incubated with appropriate dilutions of antibodies in blocking buffer at 4°C overnight, the expression of COL II (GB13021, Servicebio, 1:100), Sclerostin (Sost, SAB1307103, Sigma, 1:100), OCN(G11233, Servicebio, 1:500), TNF-α (60291–1-Ig, Sanying, 1:500), RANKL (Bs-1134R, Boaosen, 1:100), and OPG (Sc-8468, Santa Cruz, 1:200) were evaluated using immunohistochemistry. Horse Reddish Peroxidase (HRP)-labeled secondary antibody was used for 50 mins at room temperature. Color was developed using diaminobenzidine (DAB, G1211, Servicebio) as substrate. Hematoxylin (G1004, Servicbio) was used for nuclear staining. Images were captured under microscope (Nikon, #80i), Image-Pro Plus software (Media Cybernetics) was used to analyse mean density in each ROI. Integral optical density (IOD) was measured, mean density = IOD/ROI area (n=3–9/group).

Statistical analysis

Statistical analysis was performed using GraphPad Prism5 statistics software (GraphPad). Data were expressed as mean ± SD. One-way ANOVA was used to compare among the three strains followed Tukey's multiple comparision test. A value of $P < 0.05$ was considered as statistically significant.

Results

Hemichannels promote the new bone formation of callus during fracture healing

Micro-CT analysis showed that the new bone mass of callus in R76W mice were significantly increased compared to WT and Δ130–136 mice at 28th day after fracture, and there was no difference between WT and Δ130–136 mice (Fig. 1B). However, BV/TV and TMD of Δ130–136 mice were significantly increased compared to R76W mice at 28th day after fracture (Fig. 1C,D). Meanwhile, the Tb.Th of callus of Δ130–136 mice were significantly increased compared to WT and R76W mice at 14th day after fracture (Fig. 1H), and BV, Tb.Sp, and Tb.N were similar in three strains (Fig. 1E-G). Besides, three-point bending assay showed that maximal force and stiffness coefficient of tibia at 21st and 28th days after fracture were not significantly changed (Fig.1 I,J). Taken together, these results suggest that hemichannels promote the new bone formation of callus during the fracture healing, but not affect the mechanical property of healed bone.

Cx43 channels don't affect the area of callus and cartilage during fracture healing

The tibial safranin and fast green staining indicated that the cartilage area was gradually decreased, and mineralized bone gradually increased along with the process of fracture healing (Fig. 2A). The results of histological analysis revealed that the callus area and cartilage/callus ratio were not significantly different in three kinds of mice at all time points (7th, 14th, 21st and 28th days after fracture) (Fig. 2B, C). The results suggest that

hemichannels and gap junctions don't affect the ratio of intramembranous and endochondral ossification in the fracture site.

Blocking gap junctions delays the bone repair process

To investigate osteoclastogenesis during fracture healing, we measured the number of osteoclasts (Oc.S/BS) in callus at different time points (7^{th}, 14^{th}, 21^{st} and 28^{th} days) after fracture (Fig. 3A). At 21 days post-fracture, the number of osteoclasts peaked both in WT and transgenic mice, and then at 28 days post-fracture there was a significantly increased TRAP+ osteoclasts in Δ130–136 mice compared to WT and R76W mice. However, there was no obvious difference between R76W and WT mice (Fig. 3B). Observing the whole healing process, in R76W and WT mice the osteoclastogenesis reached the peak at 21st, then quickly decreased at 28^{th}, but still maintained in a high level in Δ130–136 mice at 28^{th} day.

Moreover, immunohistochemistry was used to determine the expression of key factors regulating the fracture healing of different phases in the callus. The results showed that no significant difference was detected for the expression of RANKL and OPG (Fig. 3C-F), however the expression of RANKL/OPG ratio obviously increased in Δ130–136 than WT mice at 28^{th} day (remodeling phase) after fracture (Fig. 3G). Besides, expression of sclerostin (Sost), a negative regulator of bone formation, was higher in Δ130–136 than WT mice at 14^{th} day after fracture (Fig. 3H,I).

These results showed a delay of bone repair process after blocking gap junctions, while the promotion of hemichannels in R76W may abrogate the delay.

Key regulatory factors express in advance by promoting hemichannels

The results of immunohistochemistry indicated that at 7^{th} day (inflammatory phase), expression of tumor necrosis factor (TNF)-α in R76W mice was significantly increased, and then decreased to a similar level at 14^{th} and 21^{th} day post-fracture, which indicated an enhancement of inflammatory response (Fig. 4A,B). Col II (collagen II), a key indicator of chondrogenesis, showed an increased trend at 7^{th}, and then decreased to a lower level at 14^{th} day (cartilaginous callus formation phase) than WT and Δ130–136 mice (Fig. 4C,D). Meanwhile, the expression of osteocalcin (OCN), a key regulatory factor of bone formation, was significantly increased in R76W mice at day 21 post-fracture (mineralization of callus phase), also decreased to similar level at 28 day compared with WT and Δ130–136 mice (Fig. 4E,F). Observing the whole curve, these key regulatory factors expressed in advance in R76W than WT and Δ130–136 mice, the results suggest an acceleration of fracture healing caused by promoting hemichannels in R76W mice.

Discussion

In the study, two transgenic mouse models R76W and Δ130–136 were used to determine the function of osteocytic gap junctions and hemichannels in fracture healing.

Previous studies have shown that Cx43 expression is significantly elevated in callus of WT mice(A. E. Loiselle, Lloyd, Paul, Lewis, & Donahue, 2013), and loss of Cx43 in mature

osteoblasts/osteocytes, both in osteocalcin-Cre+ and Col1-Cre+ Cx43 mice, results in delayed bone formation and fracture healing(A. E. Loiselle et al., 2013; Alayna E. Loiselle, Paul, Lewis, & Donahue). These studies identify that osteoblastic Cx43 involves in regulating the process of bone repair. However, the role of osteocytic Cx43 in fracture healing is not very clear.

Our previous studies have illustrated that Cx43 formed gap junction channel and hemichnnel in osteocytes show distinctive roles for the development and homeostasis of bone. Δ130–136 mice show significant increase in bone mineral density and corrtical thickness compared with WT and R76W mice, whereas R76W mice express higher serum bone remodeling markers (Xu et al., 2015). In the study, we generated tibial fracture, and observed an obvious promotion of new bone formation in the callus of R76W mice, whereas a delayed expression of factors regulating bone repair process in Δ130–136 mice. These results show promotion of hemichannels play some positive role, while inhibition of gap junctions play some negative role in fracture healing *in vivo.*

Consistent with increasing of new bone formation, the peak expression of TNF-α and OCN were in advance in R76W fractures relative to WT and Δ130–136 mice, which means the promotion of inflammation and osteogenesis phase in fracture healing. Because there was not obvious difference between WT and Δ130–136, we think that the main reason should be the promotion of hemichannel function in R76W. Our previous study has shown that in R76W mice the bone remodeling markers P1NP and CTX are elevated(Xu et al., 2015). Many in vitro studies have also shown that the increased opening of hemichannel promotes the release of ATP(Genetos, Kephart, Zhang, Yellowley, & Donahue, 2007) and prostaglandin E2 (PGE2)(Cherian et al., 2005; Siller-Jackson et al., 2008) in osteocytes, which can directly regulate downstream signaling and affect the function of osteoblasts to promote osteogenesis (Burra & Jiang, 2009; Jiang & Cherian, 2003).

Also, we observed an increase of Tb.Th at 14^{th} day and BV/TV and TMD in whole callus in Δ130–136 mice at 28^{th} day post fracture in this study. We think that is due to the higher baseline of tibial cortical BMD and BV/TV in Δ130–136 mice than WT and R76W(Xu et al., 2015), the lower baseline neutralized the influence of increased new bone in R76W on the whole callus.

In addition to bone formation, bone resorption is also important for the remodeling of impaired bone. In the study, Δ130–136 showed an obvious increased osteoclast area at 28^{th} day after fracture, which was consistant with the increase of RANKL/OPG, the principal mediators of osteoclastogenesis(Yasuda et al., 1998). The peak osteoclast area in callus of WT and R76W mice was at 21 days post fracture, then declined to lower level at 28 days, however in Δ130–136 the osteoclast area still remained in a high level till 28 days. We think that may indicate a delay of osteoclast-drived-remodeling phase in healing process in Δ130–136. Alayna E. Loiselle et al have also showed that the peak osteoclast number appear at 28 days in WT, but at 35 days in Col1-Cre Cx43cKO fractures(A. E. Loiselle et al., 2013). Osteocytes send signals to the osteoclasts providing information on where to resorb and repair(Schaffler, Cheung, Majeska, & Kennedy, 2014). Osteocyte apoptosis precede and recruit osteoclasts and initiate bone resorption(Aguirre et al., 2006; Verborgt, Gibson, &

Schaffler, 2000). Osteocytic Cx43-formed channels are important for communication between osteocytes and osteoclasts and subsequent osteoclastogenesis and remodeling(Middleton, Al-Dujaili, Mei, Gunther, & You, 2017; Wu, Zhou, Huang, Ji, & Kang, 2017). We think that inhibition of Cx43-formed-channels influences the release of regulatory factors and then the function of osteoblasts and osteoclasts(Buo, Tomlinson, Eidelman, Chason, & Stains, 2017), in turn retard the bone healing. Moreover, in the study, no significant difference was found in osteoclast area between WT and R76W, which may be owing to that promotion of hemichannels in R76W counteracts the delay of osteoclastogenesis caused by gap junction inhibition. Also, we have found that PGE2 release in serum of R76W significantly increased than that of WT and Δ130–136 mice (data not shown).

In the study, we observed an obvious increase of Sost expression at 14th day in Δ130–136, which was also observed in Cx43cKO fractures(A. E. Loiselle et al., 2013). Sost have a catabolic action on bone through the promotion of osteoclast formation(Wijenayaka et al., 2012) and the inhibition of bone formation(Qin et al., 2015) by regulating Wnt signaling. Cx43 is involved in regulating(Bivi et al., 2012) and also being regulated by Wnt/β-catenin signaling(Xia et al., 2010). Alayna E. Loiselle et al have shown the attenuated β-catenin expression in the case of Cx43 deficiency(A. E.Loiselle et al., 2013), which should be another reason for the delay of healing in Δ130–136 mice.

In conclusion, we have shown that impairment of Cx43-formed-gap junctions in osteocytes delays osteoclastogenesis of fracture repair, while promotion of hemichannels increases new bone formation of callus by accelerating healing process. The delay of healing caused by gap junctions may be recovered by hemichannel promotion. These results show that gap junctions and hemichannels may play some similar and cooperative roles in bone repair. Maintaining normal function of Cx43-formed channels is important for fracture healing.

Also, we think the shortcomings of the present study are that more time-points after 28 days (such as 35 days post fracture) should be analyzed to observe whether the dalayed healing can be restored in Δ130–136 mice. That will be better for understanding the roles of channels in bone repair.

ACKNOWLEDGMENTS

This work was supported by the National Natural Science Foundation of China (Nos. 81472090 and 81772409) and grants from the National Institutes of Health (No. AG045040) and Welch Foundation (No. AQ-1507).

Funding information

National Natural Science Foundation of China, Grant/Award Numbers: 81472090, 81772409; National Institutes of Health, Grant/Award Numbers: AG045040; Welch Foundation, Grant/Award Numbers: AQ-1507.

REFERENCES:

Aguirre JI, Plotkin LI, Stewart SA, Weinstein RS, Parfitt AM, Manolagas SC, & Bellido T (2006). Osteocyte apoptosis is induced by weightlessness in mice and precedes osteoclast recruitment and bone loss. Journal of Bone and Mineral Research, 21(4), 605–615. 10.1359/jbmr.060107 [PubMed: 16598381]

Batra N, Kar R, & Jiang JX (2012). Gap junctions and hemichannels in signal transmission, function and development of bone. Biochim Biophys Acta, 1818(8), 1909–1918. 10.1016/j.bbamem.2011.09.018 [PubMed: 21963408]

Bivi N, Condon KW, Allen MR, Farlow N, Passeri G, Brun LR, …Plotkin LI (2012). Cell autonomous requirement of connexin 43 for osteocyte survival: consequences for endocortical resorption and periosteal bone formation. J Bone Miner Res, 27(2), 374–389. 10.1002/jbmr.548 [PubMed: 22028311]

Bonewald LF, Kneissel M, & Johnson M (2013). Preface: the osteocyte. Bone, 54(2), 181 10.1016/j.bone.2013.02.018 [PubMed: 23486185]

Buo AM, Tomlinson RE, Eidelman ER, Chason M, & Stains JP (2017). Connexin43 and Runx2 interact to affect cortical bone geometry, Skeletal Development, and Osteoblast and Osteoclast Function. J Bone Miner Res. 32(8), 1727–1738. 10.1002/jbmr.3152 [PubMed: 28419546]

Burra S, & Jiang JX (2009). Connexin 43 hemichannel opening associated with Prostaglandin E(2) release is adaptively regulated by mechanical stimulation. Commun Integr Biol, 2(3), 239–240. [PubMed: 19641742]

Cherian PP, Siller-Jackson AJ, Gu S, Wang X, Bonewald LF, Sprague E, & Jiang JX (2005). Mechanical strain opens connexin 43 hemichannels in osteocytes: a novel mechanism for the release of prostaglandin. Mol Biol Cell, 16(7), 3100–3106. 10.1091/mbc.E04-10-0912 [PubMed: 15843434]

Civitelli R (2008). Cell-cell communication in the osteoblast/osteocyte lineage. Arch Biochem Biophys, 473(2), 188–192. 10.1016/j.abb.2008.04.005 [PubMed: 18424255]

Genetos DC, Kephart CJ, Zhang Y, Yellowley CE, & Donahue HJ (2007). Oscillating fluid flow activation of gap junction hemichannels induces atp release from MLO-Y4 osteocytes. Journal of Cellular Physiology, 212(1), 207–214. 10.1002/jcp.21021 [PubMed: 17301958]

Huang CP, Chen XM, & Chen ZQ (2008). Osteocyte: the impresario in the electrical stimulation for bone fracture healing. Med Hypotheses, 70(2), 287–290. 10.1016/j.mehy.2007.05.044 [PubMed: 17689020]

Jawad MU, Fritton KE, Ma T, Ren PG, Goodman SB, Ke HZ, …Genovese MC (2013). Effects of sclerostin antibody on healing of a non-critical size femoral bone defect. J Orthop Res, 31(1), 155–163. 10.1002/jor.22186 [PubMed: 22887736]

Jiang JX, & Cherian PP (2003). Hemichannels formed by connexin 43 play an important role in the release of prostaglandin E(2) by osteocytes in response to mechanical strain. Cell Commun Adhes, 10(4–6), 259–264. 10.1080/15419060390262994 [PubMed: 14681026]

Kusuzaki K, Kageyama N, Shinjo H, Takeshita H, Murata H, Hashiguchi S, …Hirasawa Y (2000). Development of bone canaliculi during bone repair. Bone, 27(5), 655–659. 10.1016/S8756-3282(00)00383-5 [PubMed: 11062352]

Li C, Ominsky MS, Tan HL, Barrero M, Niu QT, Asuncion FJ, …Ke HZ (2011). Increased callus mass and enhanced strength during fracture healing in mice lacking the sclerostin gene. Bone, 49(6), 1178–1185. 10.1016/j.bone.2011.08.012 [PubMed: 21890008]

Loiselle AE, Lloyd SA, Paul EM, Lewis GS, & Donahue HJ (2013). Inhibition of GSK-3beta rescues the impairments in bone formation and mechanical properties associated with fracture healing in osteoblast selective connexin 43 deficient mice. PLoS One, 8(11), e81399 10.1371/journal.pone.0081399 [PubMed: 24260576]

Loiselle AE, Paul EM, Lewis GS, & Donahue HJ Osteoblast and osteocyte-specific loss of Connexin43 results in delayed bone formation and healing during murine fracture healing. Journal of Orthopaedic Research, 31(1):147–154. 10.1002/jor.22178

Marsell R, & Einhorn TA (2011). The biology of fracture healing. Injury, 42(6), 551–555. 10.1016/j.injury.2011.03.031 [PubMed: 21489527]

McGee-Lawrence ME, Ryan ZC, Carpio LR, Kakar S, Westendorf JJ, & Kumar R (2013). Sclerostin deficient mice rapidly heal bone defects by activating beta-catenin and increasing intramembranous ossification. Biochem Biophys Res Commun, 441(4), 886–890. 10.1016/j.bbrc.2013.10.155 [PubMed: 24211207]

Middleton K, Al-Dujaili S, Mei X, Gunther A, & You L (2017). Microfluidic co-culture platform for investigating osteocyte-osteoclast signalling during fluid shear stress mechanostimulation. J Biomech, 59, 35–42. 10.1016/j.jbiomech.2017.05.012 [PubMed: 28552413]

Ominsky MS, Li C, Li X, Tan HL, Lee E, Barrero M, …Ke HZ (2011). Inhibition of sclerostin by monoclonal antibody enhances bone healing and improves bone density and strength of nonfractured bones. J Bone Miner Res, 26(5), 1012–1021. 10.1002/jbmr.307 [PubMed: 21542004]

Plotkin LI, & Bellido T (2013). Beyond gap junctions: Connexin43 and bone cell signaling. Bone, 52(1), 157–166. 10.1016/j.bone.2012.09.030 [PubMed: 23041511]

Qin W, Li X, Peng Y, Harlow LM, Ren Y, Wu Y, …Cardozo CC (2015). Sclerostin antibody preserves the morphology and structure of osteocytes and blocks the severe skeletal deterioration after motor-complete spinal cord injury in rats. J Bone Miner Res, 30(11), 1994–2004. 10.1002/jbmr.2549 [PubMed: 25974843]

Schaffler MB, Cheung WY, Majeska R, & Kennedy O (2014). Osteocytes: master orchestrators of bone. Calcif Tissue Int, 94(1), 5–24. 10.1007/s00223-013-9790-y [PubMed: 24042263]

Schindeler A, McDonald MM, Bokko P, & Little DG (2008). Bone remodeling during fracture repair: The cellular picture. Semin Cell Dev Biol, 19(5), 459–466. 10.1016/j.semcdb.2008.07.004 [PubMed: 18692584]

Siller-Jackson AJ, Burra S, Gu S, Xia X, Bonewald LF, Sprague E, & Jiang JX (2008). Adaptation of connexin 43-hemichannel prostaglandin release to mechanical loading. J Biol Chem, 283(39), 26374–26382. 10.1074/jbc.M803136200 [PubMed: 18676366]

Tatsuyama K, Maezawa Y, Baba H, Imamura Y, & Fukuda M (2000). Expression of various growth factors for cell proliferation and cytodifferentiation during fracture repair of bone. Eur J Histochem, 44(3), 269–278. [PubMed: 11095098]

Verborgt O, Gibson GJ, & Schaffler MB (2000). Loss of osteocyte integrity in association with microdamage and bone remodeling after fatigue in vivo. J Bone Miner Res, 15(1), 60–67. 10.1359/jbmr.2000.15.1.60 [PubMed: 10646115]

Wijenayaka AR, Kogawa M, Lim HP, Bonewald LF, Findlay DM, & Atkins GJ (2012). Sclerostin stimulates osteocyte support of osteoclast activity by a RANKL-dependent pathway. PLoS One, 6(10), e25900 10.1371/journal.pone.0025900

Wu Q, Zhou X, Huang D, Ji Y, & Kang F (2017). IL-6 Enhances Osteocyte-Mediated Osteoclastogenesis by Promoting JAK2 and RANKL Activity In Vitro. Cell Physiol Biochem, 41(4), 1360–1369. 10.1159/000465455 [PubMed: 28278513]

Xia X, Batra N, Shi Q, Bonewald LF, Sprague E, & Jiang JX (2010). Prostaglandin promotion of osteocyte gap junction function through transcriptional regulation of connexin 43 by GSK-3-{beta}-catenin signaling. Mol Cell Biol, 30(1), 206–219. 10.1128/MCB.01844-08 [PubMed: 19841066]

Xu H, Gu S, Riquelme MA, Burra S, Callaway D, Cheng H, … Jiang JX (2015). Connexin 43 channels are essential for normal bone structure and osteocyte viability. J Bone Miner Res, 30(3), 436–448. 10.1002/jbmr.2374 [PubMed: 25270829]

Yasuda H, Shima N, Nakagawa N, Yamaguchi K, Kinosaki M, Mochizuki S, …Suda T (1998). Osteoclast differentiation factor is a ligand for osteoprotegerin/osteoclastogenesis-inhibitory factor and is identical to TRANCE/RANKL. Proc Natl Acad Sci U S A, 95(7), 3597–3602. 10.1073/pnas.95.7.3597 [PubMed: 9520411]

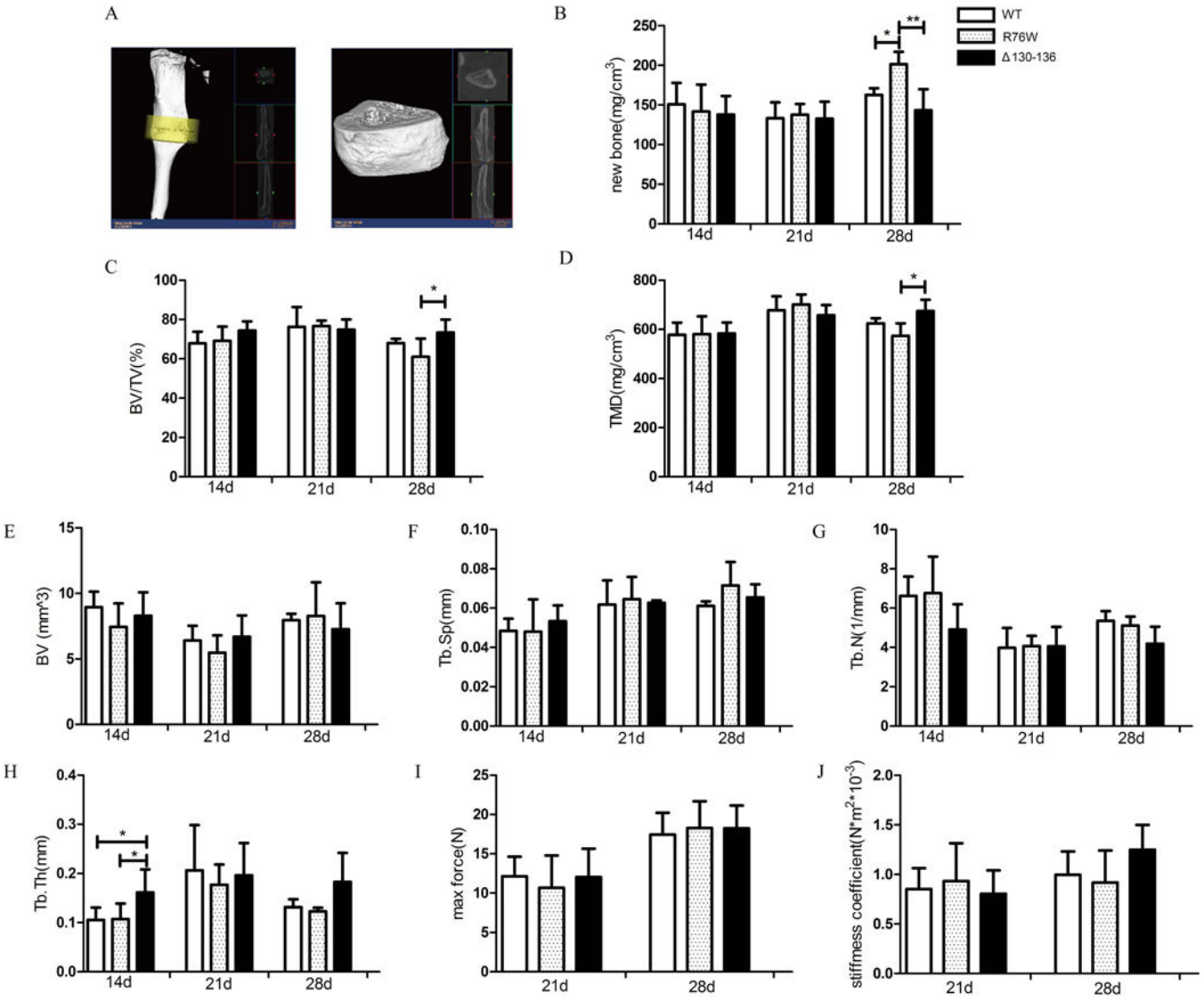

Figure 1.

Hemichannels promote the new bone formation of callus during fracture healing. (A) Micro-CT images of tibial callus, yellow area shows the region of interest (ROI) above and below the fracture line. (B) Micro-CT analysis showed that the new born bone mass in R76W mice were significantly increased compared to WT and Δ130–136 mice at 28th day after fracture. BV/TV (C) and TMD (D) of Δ130–136 mice were significantly increased compared to R76W mice at 28th day after fracture. Tb.Th (H) was significantly increased in Δ130–136 compared with that of WT and R76W mice at 14th day after fracture. BV (E), Tb.Sp (F) and Tb.N (G) were similar in all of three groups. Three-point bending assay showed that maximal force (I) and stiffness coefficient of tibia (J) at 21st and 28th days after fracture were not significantly different in three kinds of mouse models. Data shown are mean ± SD. *$p < 0.05$; ** $p < 0.01$. n=5–7. BV = Callus bone volume; BV/TV = Bone Volume to Tissue Volume; TMD = Tissue Mineral Density; Tb.Sp = Trabecular Separation; Tb.Th = Trabecular Thickness; Tb.N= Trabecular Number.

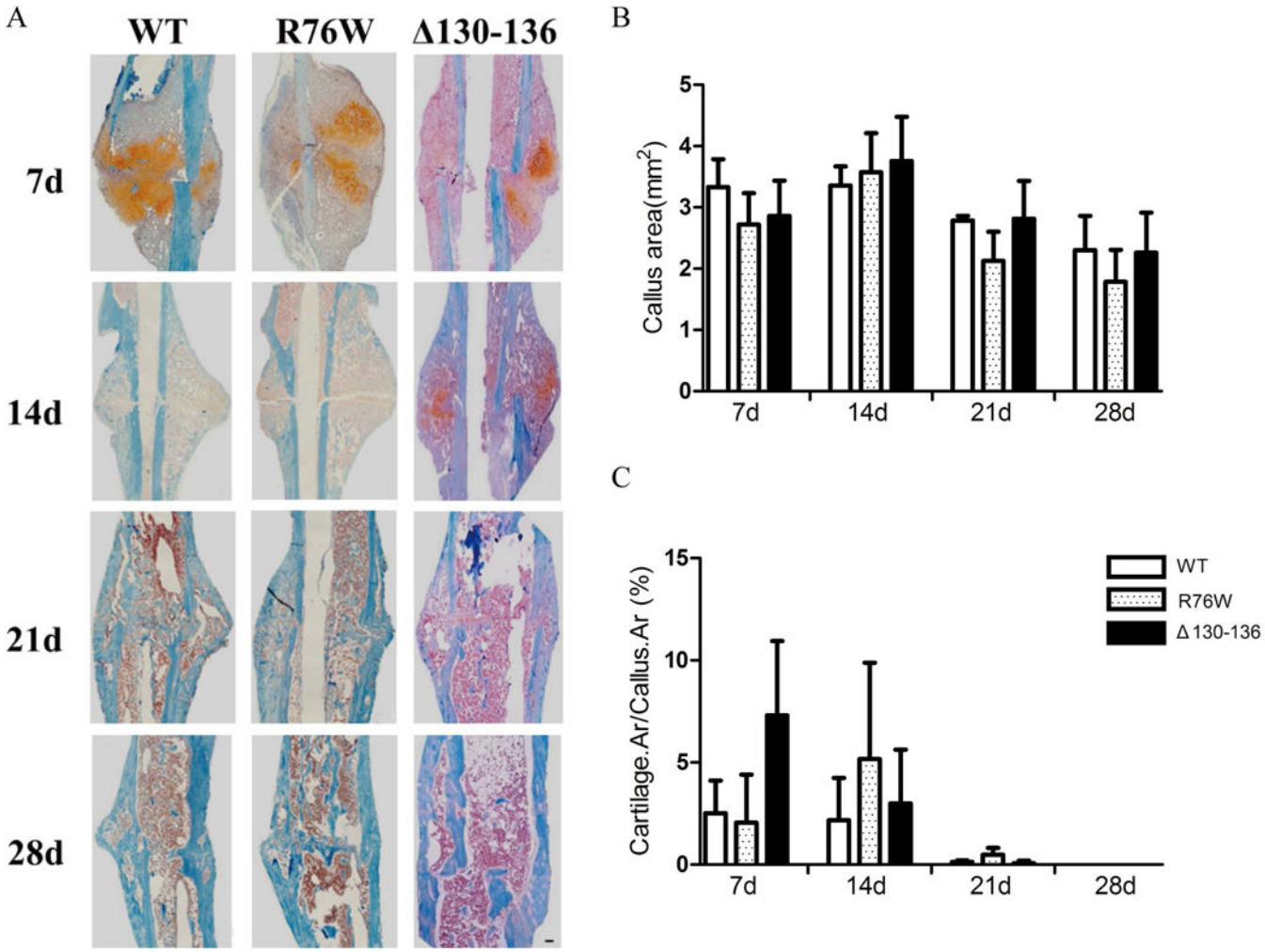

Figure 2.

Cx43 channels didn't affect the area of callus and cartilage during fracture healing. (A) Representative images of safranin and fast green staining in callus of WT, R76W and Δ130–136 mice at 7, 14, 21 and 28 days after fracture. (B) Quantification of callus area and (C) cartilage/callus ratio. Data shown are mean ± SD. n=3–6. Scale bars = 50μm.

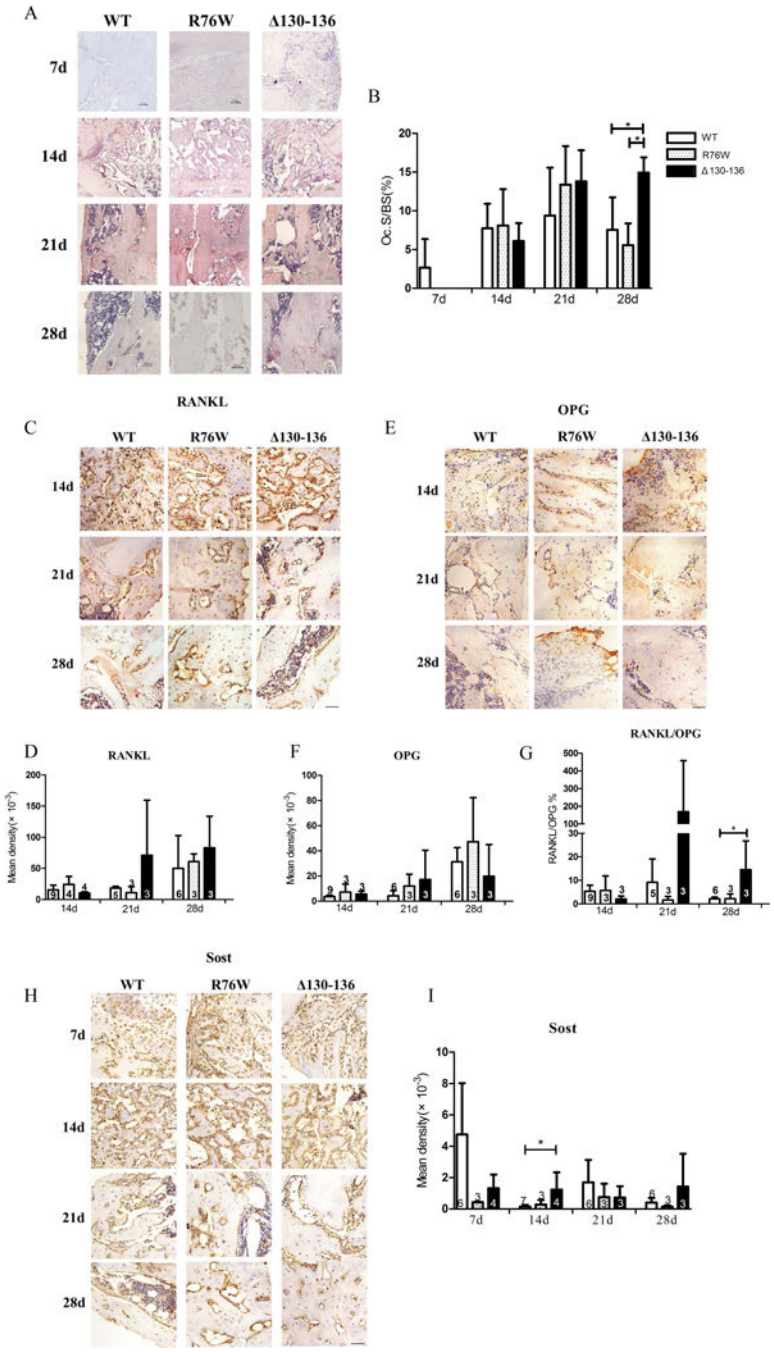

Figure 3.

Blocking gap junctions delayed the bone repair process. (A) Representative images of TRAP staining in callus of WT, R76W and Δ130–136 mice at 7, 14, 21 and 28 days after fracture. (B) Quantification of TRAP+ osteoclasts (Oc.S/BS) in callus. Representative images of RANKL (C), OPG (E) and Sost (H) immunostaining in callus of WT, R76W and Δ130–136 mice after fracture. Quantification of RANKL (D), OPG (F), Sost (I) expression and ratio of RANKL/OPG (G). Data shown are mean ± SD. *$p < 0.05$. n=3–9. RANKL = Receptor

Activator for Nuclear Factor-κB Ligand; OPG = osteoprotegerin; Sost = sclerostin. Scale bars = 50μm.

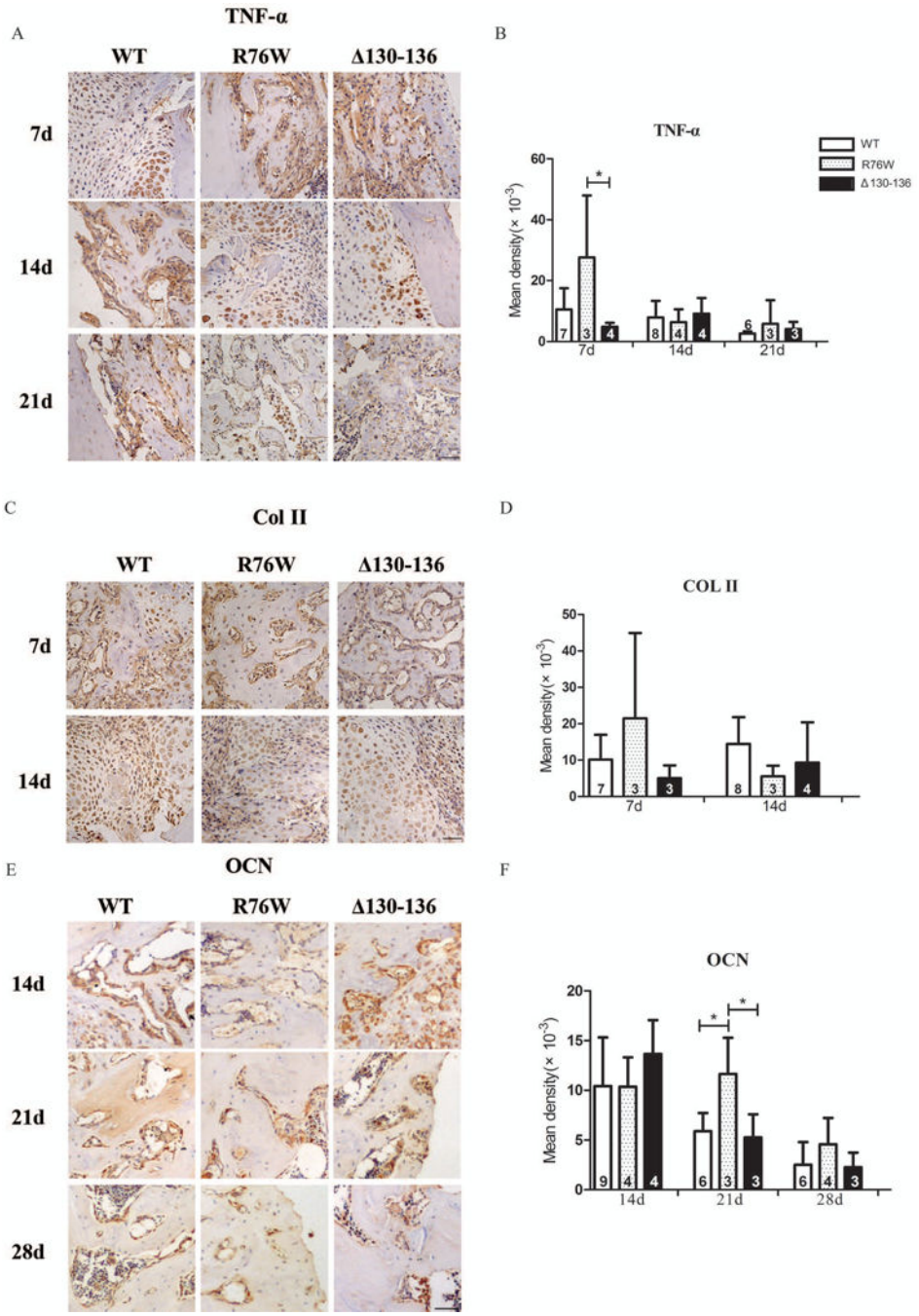

Figure 4.

Key regulatory factors express in advance by promoting hemichannels. Representative images of TNF-α (A), Col II (C), OCN (E), immunostaining in callus of WT, R76W and Δ130–136 mice after fracture. Quantification of TNF-α (B), Col II (D) and OCN (F) expression. Data shown are mean ± SD. *$p < 0.05$. n=3–9. TNF-α = tumor necrosis factor-α; Col II = Collagen II; OCN = osteocalcin. Scale bars = 50μm.